communications
earth & environment

ARTICLE

https://doi.org/10.1038/s43247-022-00609-0 OPEN

Spatially consistent microbial biomass and future cellular carbon release from melting Northern Hemisphere glacier surfaces

Ian T. Stevens [1,2]✉, Tristram D. L. Irvine-Fynn [2], Arwyn Edwards[3], Andrew C. Mitchell [2], Joseph M. Cook[1], Philip R. Porter [4], Tom O. Holt [2], Matthias Huss[5,6,7], Xavier Fettweis [8], Brian J. Moorman [9], Birgit Sattler [10] & Andy J. Hodson [11,12]

Melting glacier ice surfaces host active microbial communities that enhance glacial melt, contribute to biogeochemical cycling, and nourish downstream ecosystems; but these communities remain poorly characterised. Over the coming decades, the forecast 'peak melt' of Earth's glaciers necessitates an improvement in understanding the state and fate of supraglacial ecosystems to better predict the effects of climate change upon glacial surfaces and catchment biogeochemistry. Here we show a regionally consistent mean microbial abundance of 10^4 cells mL^{-1} in surface meltwaters from eight glaciers across Europe and North America, and two sites in western Greenland. Microbial abundance is correlated with suspended sediment concentration, but not with ice surface hydraulic properties. We forecast that release of these microbes from surfaces under a medium carbon emission scenario (RCP 4.5) will deliver 2.9×10^{22} cells yr^{-1}, equivalent to 0.65 million tonnes yr^{-1} of cellular carbon, to downstream ecosystems over the next ~80 years.

[1] Department of Environmental Science, Aarhus University, 4000 Roskilde, Denmark. [2] Department of Geography and Earth Sciences, Aberystwyth University, Aberystwyth SY23 3DB, UK. [3] Institute of Biological, Environmental and Rural Sciences, Aberystwyth University, Aberystwyth SY23 3DA, UK. [4] Geography, Environment and Agriculture, School of Life and Medical Sciences, University of Hertfordshire, Hatfield AL10 9AB, UK. [5] Laboratory of Hydraulics, Hydrology and Glaciology (VAW), ETH Zürich, 8049 Zürich, Switzerland. [6] Swiss Federal Institute for Forest, Snow and Landscape Research WSL, 8903 Birmensdorf, Switzerland. [7] Department of Geosciences, University of Fribourg, 1700 Fribourg, Switzerland. [8] Department of Geography, University of Liege, 4000 Liege, Belgium. [9] Department of Geography, University of Calgary, Calgary T2N 1N4 AB, Canada. [10] Department of Ecology, University of Innsbruck, Austrian Polar Research Institute, 6200 Innsbruck, Austria. [11] Arctic Geology, The University Centre in Svalbard (UNIS), 9171 Longyearbyen, Svalbard, Norway. [12] Department of Environmental Science, Western Norway University of Applied Sciences, 6856 Songdal, Norway. ✉email: ian.stevens@envs.au.dk

Earth's glaciers and ice sheets are melting at a rate of ~780 Gt yr^{-1} (ref. [1]) and consequently are delivering meltwater, microbes, nutrients and sediment into aquatic, terrestrial and marine environments. The loss of ice from glaciers outside Greenland and Antarctica is accelerating[2] and is expected to peak within the next 50 years[3]. This meltwater discharge will have profound effects upon the microbial productivity, biogeochemical cycles, and biodiversity and function[4] of glacier-fed ecosystems[5,6]. Of particular importance is the organic carbon (OC) that these glacial meltwaters deliver to downstream environments[7,8], supplementing these locations with bioavailable OC[9]. Fluctuations in OC delivery from glaciers can, however, result in complex ecological responses in mountain waters[10]. One component of glacially-derived OC is the active microbial ecosystem found on melting glacier surfaces[11], which furnishes meltwater with dissolved and particulate organic carbon (DOC and POC respectively) and microbial assemblages[12–14]. In Greenland, recent estimates suggest 250 g km^{-2} of cellular carbon is released each day from the ice surface to supraglacial streams[15], but no equivalent assessments exist for any other glaciers or ice sheets.

On the ice surface, the so-called 'weathering crust'[16] offers a variety of microbial habitats in saturated and unsaturated subsurface ice and within the cryoconite holes that punctuate the ice surface[17] (Fig. 1). This extensive, near-surface interfluve photic zone[18] is formed during the melt season as exposed glacier ice develops a shallow (<2 m) porous surface layer in response to shortwave radiation penetration into the subsurface[16]. It is rich in aeolian and emergent abiotic and biotic particles, cryoconite, and nutrient-bearing liquid meltwater, which supports an extensive microbial community including photoautotrophic ice algae and cyanobacteria, bacterial heterotrophs and other protists[19]. Despite estimates of ~10^{26} microbial cells harboured within Earth's seasonally exposed weathering crust ecosystem[18], assessments of community activity[20] and associated production, storage and transfer of OC[21,22] across glacier ice surfaces remain sparse. The hydrologically active weathering crust[23,24] connects the glacier surface habitats with downstream environments via the supra-, en- and sub-glacial hydrological networks[13]; yet this hydraulic connection, and its role in regulating the transport of biomass and OC across the surface of mountain glaciers, remains poorly understood.

The contemporary relevance of biomass transfer from glacier surfaces is amplified in this 'peak melt' century. During the 21st century air temperature rise will drive an expansion of bare-ice melt area and increase in glacial runoff, before both decline as glaciers recede across the European Alps[25] and European and North American Arctic[26,27]. The associated expansion and contraction of melting weathering crust areas will regulate the cycling of supraglacial OC and its delivery to glacier-fed ecosystems[7]. To establish understanding of these fundamental processes, we evaluate microbe abundance in glacial weathering crust meltwaters, and examine its association with supraglacial hydraulic properties across contrasting latitudinal and climatological settings from eight northern hemisphere glaciers and two sites on the Greenland Ice Sheet (Fig. 2, Supplementary Table 2). We

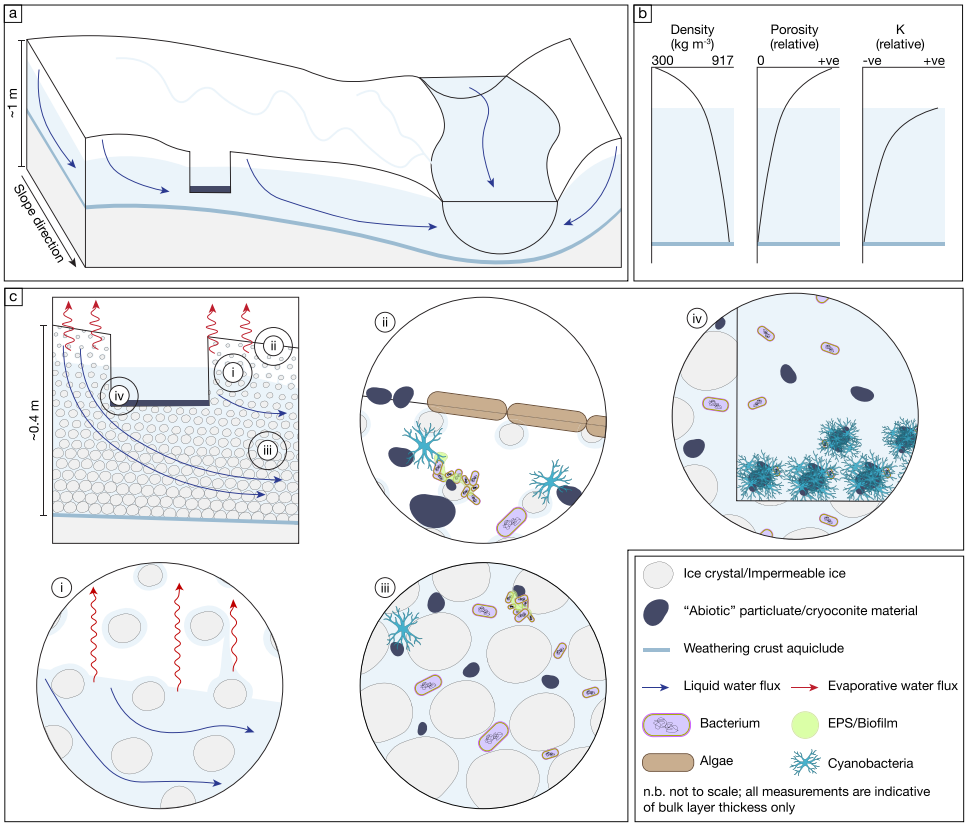

Fig. 1 A conceptual model of the glacial weathering crust. a A catchment-scale transect and water flow across and beneath the ice surface, for which **b** indicative depth-variable relationships for bulk ice density, porosity and hydraulic conductivity (*K*) are shown. **c** Insets depict exemplar meltwater-saturated or unsaturated microbial habitats or niches: i) shows the near-surface unsaturated zone with capillary draw and evaporative water fluxes; ii) illustrates the highly porous ice-atmosphere interface where glacier ice algae thrive; iii) portrays the saturated weathering crust zone; and iv) represents a cryoconite hole ecosystem that punctuates the weathering crust, hosting a one-particle thick layer of cryoconite granules. Microbes suspected to be present in each environmental niche are indicated.

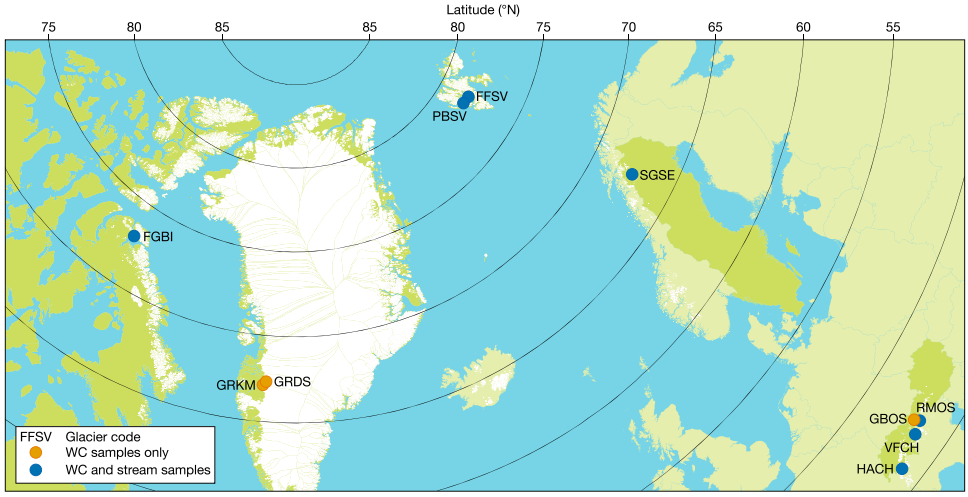

Fig. 2 Supraglacial sampling sites distributed around the Northern Hemisphere. Glacier codes are as follows: FFSV: Foxfonna; FGBI: Fountain Glacier; GBOS: Gaisbergferner; GRDS: Greenland Ice Sheet (S6); GRKM: Greenland Ice Sheet (Point 660); HACH: Haut Glacier d'Arolla; PBSV: Protektorbreen; RMOS: Rotmoosferner; SGSE: Storglaciären; and VFCH: Vadrec del Forno. Metadata for each site can be found in Supplementary Table 2.

reveal a mean microbial abundance of 10^4 cells mL^{-1}, a maximum of 10^5 cells mL^{-1}, and demonstrate the importance of the supraglacial ecosystem in delivering microbes to downstream environments in the coming eight decades. The study provides a benchmark assessment of supraglacial cell concentrations and biomass on North American and European glacier surfaces and presents a first order estimate of the contribution this system makes to global OC fluxes.

Results and discussion

The microbial abundance of glacier surfaces. Our optimised flow cytometry protocol (as outlined in the Supplementary Information) was employed on 763 weathering crust meltwater samples and revealed a mean microbial abundance of $2.2 \times 10^4 \pm 5.5 \times 10^4$ cells mL^{-1} (Figs. 3 and 4). In contrast, other aquatic and terrestrial habitats typically have higher cell concentrations: upper (<200 m depth) ocean waters contain 10^5 cells mL^{-1}; lower (>200 m depth) ocean waters 10^4 cells mL^{-1}; freshwaters 10^6 cells mL^{-1}; and 10^{7-8} cells cm^{-3} in the upper 10 m of unconsolidated terrestrial sediments[28]. Moreover, other cryosphere systems also exhibit higher microbial abunace than supraglacial meltwaters, for example: snow – 10^5 cells mL^{-1} (ref. [29]); sea ice and lake ice (both 10^6 cells mL^{-1} (refs. [30,31])); and the subglacial environment 10^5 cells mL^{-1} (ref. [32]).

We show no significant statistical difference between weathering crust abundance and 142 equivalent in-stream abundance of $2.2 \times 10^4 \pm 3.0 \times 10^4$ cells mL^{-1} (details of all statistical testing are summarised in Supplementary Table 4); a phenomenon which is replicated when samples are examined on a site-by-site basis (Supplementary Table 4). These meltwater abundances correspond well to those reported in the previous Arctic and Alpine work (10^3–10^5 cells mL^{-1})[33–35]. However, the abundances we describe are typically lower than those reported for glacial surface ice 10^{4-6} cells mL^{-1} (refs. [35–37]), but equivalent to cryoconite hole waters (~10^4 cells mL^{-1} (refs. [38–41])), which are hydrologically connected with the weathering crust (Fig. 1, ref. [24]). A simplistic comparison of these concentrations implies that, once removed from the melting ice surface, microbes are entrained in weathering crust meltwaters and efficiently advected to the supraglacial stream network. Beyond this simple numeric comparison, future studies should look to focus on the role of cryoconite holes in this process, and interaction with the particulate layer found at the base of such holes.

There are, however, significant differences in weathering crust cell concentrations between glaciers (Supplementary Table 3) with pairwise comparisons revealing significantly higher abundance in Greenland's Dark Zone (mean cell concentration of 4.7×10^4 cells mL^{-1}) than reported for the European Alpine glaciers of Haut Glacier d'Arolla, Vadrec del Forno and Rotmoosferner and the sub-arctic Storglaciären, where mean abundances range from 2.9 to 3.9×10^4 cells mL^{-1} (Fig. 3 and Supplementary Table 5A). In-stream abundances also differ between glaciers (Supplementary Table 3), with a significant pairwise contrast between Fountain Glacier, Canada, (3.6×10^4 cells mL^{-1}) and Vadrec del Forno, Switzerland, (1.5×10^4 cells mL^{-1}; Supplementary Table 5B). Critically, despite these differences, mean microbial abundances are within the same order of magnitude (10^4 cells mL^{-1}) in both weathering crust and stream meltwaters across all sample locations.

The modal size class of meltwater borne microbes is 1–2 µm ($n = 905$), containing 53.1 ± 8.8 % of the enumerated microbes; whilst 71.7% of the microbes were ≤2 µm, and 86.3% ≤4 µm (Fig. 3). Microbes exceeding 10 µm (thereafter large cells), most likely being cyanobacteria or eukaryotic algae[15], on average comprise 13.5%, equivalent to an absolute abundance of 2.9×10^3 cells mL^{-1}, of total microbes. Notably, as microbial size distributions within the weathering crust and supraglacial stream meltwaters are comparable at all glaciers and when considering the dataset in its entirety (Fig. 2).

Controls upon microbial abundance and biomass transport. We pair 614 microbial abundance measurements with corresponding hydrological data, including: weathering crust hydraulic conductivity (K), water table depth relative to the ice surface[23]; electrical conductivity (EC, a proxy for total solute concentration); water temperature; and, for 90 stream samples, meltwater discharge (Q). Moreover, suspended sediment concentration was measured for all 905 abundance records by enumerating non-stained particles (i.e., those excluded from the cell gate) in each cytogram. Across the hemispheric dataset, the variable which correlates most strongly with microbial abundance is suspended sediment concentration (Supplementary Table 3); with the examination of this relationship on a glacier-by-glacier basis revealing stronger model fits (Fig. 4).

Regression model fits between measured hydraulic variables are not statistically significant (Fig. 4, Supplementary Table 3).

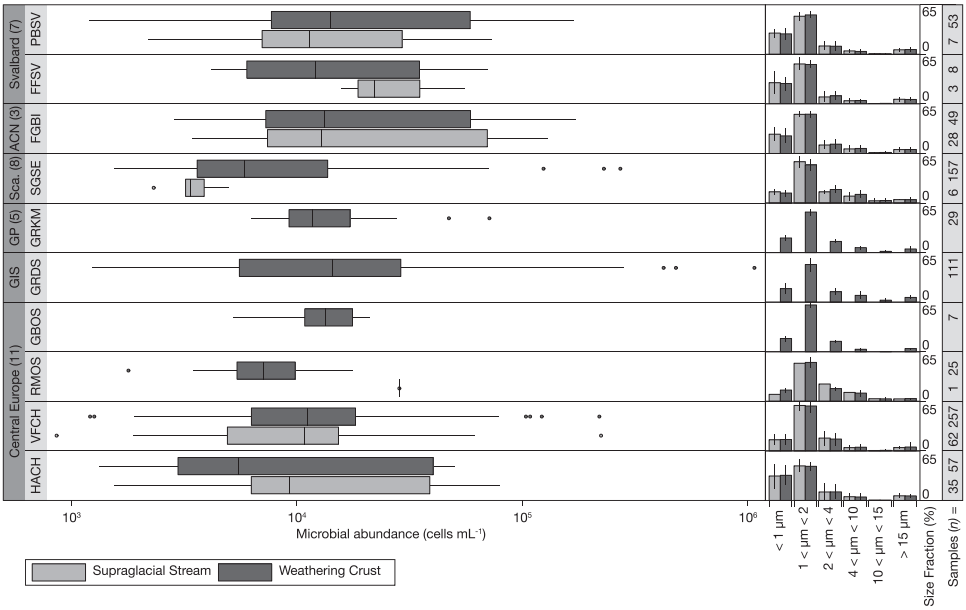

Fig. 3 Cell concentration and size distributions within the weathering crust and supraglacial streams at each investigated glacier. All distributions are box and whisker plots displaying median, 25 to 75 percentiles, distribution range and outlying sample measurements (as grey dots) for each glacier in latitudinal order (from north to south). Each site is coded by RGI region (ACN: Arctic Canada North; Sca.: Scandinavia; GP: Greenland Periphery and GIS: Greenland Ice Sheet; and glacier identifier (listed in Fig. 2). Sample numbers (*n*) correspond to the abundance box plots with which they vertically align.

However, at the glacier-scale, contrasts exist, with examples of weak inverse relationships between *K* and cell concentration at sites in western Greenland and positive associations found at Gaisbergferner (Austria) and Fountain Glacier. EC and water temperature demonstrate significant relationships with cell concentration but have poor model fits ($r^2 < 0.04$) with cell concentration (Supplementary Table 3). Our data suggest that across five orders of magnitude in hydraulic conductivity (10^{-3}–10^{1} m d^{-1}) and three orders of magnitude in stream discharge (10^{-3}–10^{0} m^3 s^{-1}), microbial abundance in glacial meltwater is broadly stable with 97% of our samples in the order 10^4 cells mL^{-1} ($n = 905$). This ostensible lack of a clear, dominant, or consistent association between abundance and hydrological variables implies that alternate, ecological or glaciological factors must regulate the microbe numbers in weathering crust meltwaters.

The weak, positive relationship between microbial and suspended sediment concentrations may explain the relatively high abundances we report in Greenland's Dark Zone; an area rich in such particulates[42,43]. This relationship may simply reflect that sediment and cells are mobilised under the same hydrological conditions or may be due to the presence of sediment liberated from suspended microbial aggregates (which are disaggregated as part of our cytometric method). Within such aggregates, sediment particles may offer loci for microbe attachment and/or a supply of scavenged nutrients such as bio-mined phophorus[44]. Alternate ecological controls upon microbial abundance may include: (i) specific nutrient availability (e.g. nitrogen[45] and/or phosphorus[44]), and/or (ii) mortality controls such as predation or viral lysis[46], and photo-degradation and/or photolysis[47], which all present avenues for future investigation.

The combination of low hydraulic conductivity (<1 m d^{-1}) and typical supraglacial stream spacing[48,49] implies interfluvial transit times that exceed reported community doubling times on glaciers (1–11 days[20,39,46]). However, our data reveal that the biomass transiting through the weathering crust across a range of melt regimes and surface geometries is broadly consistent and stable, implying that replication either does not occur in weathering crust meltwaters or is rate-matched by the limiting factors considered above. To further elucidate this potential control on cell concentration, future research should look to examine the active, dormant, damaged or dead fractions of these microbes, their levels of activity and contribution to the broader supraglacial and downstream ecosystems[50].

The varied and continually changing structure[51], pore geometry and porosity[16] of ablating glacier ice invites further assessment of its role in regulating cell concentration and transport. The proportion, sizes and biomass of cells that are immobile within the weathering crust ice matrix remains unclear: whether entombed within solid ice crystals[40], resident in low shear havens such as disconnected pores, ice crystal-bound water[52], or the unsaturated zone of the weathering crust[23,53]; retained between crystals via mechanical filtration[34]; or bound to crystals by extra-cellular polymeric substances (EPS)[54], ice binding proteins[55], or biofilms[56]. Future work, especially considering the accumulation of microbes within the weathering crust[15], or so-called 'biological albedo reduction'[57], should examine and characterise these potential controls on microbial abundance and cell retention.

The export and contribution of weathering crust microbes to global carbon cycling during the 21st century. By coupling our regionally consistent microbial abundance and cell size distribution assessments with predicted glacier ice melt volumes, we provide a conservative, first order forecast of annual regional microbial cell and carbon export from glacier surfaces over the coming century. We use global circulation model driven projections for Randolph Glacier Inventory (RGI)[58] regions 1-12 (i.e. the Northern Hemisphere excluding High Mountain Asia, thereafter: glaciers) under low, medium and high emissions scenarios (Representative Concentration Pathways (RCP) 2.6, 4.5 and 8.5 respectively)[59] and the Greenland Ice Sheet under medium and high scenarios[60]. Cellular carbon content per unit meltwater volume was calculated using abundance-size derived cell biovolume and allometric conversion ratios[61,62]. In the

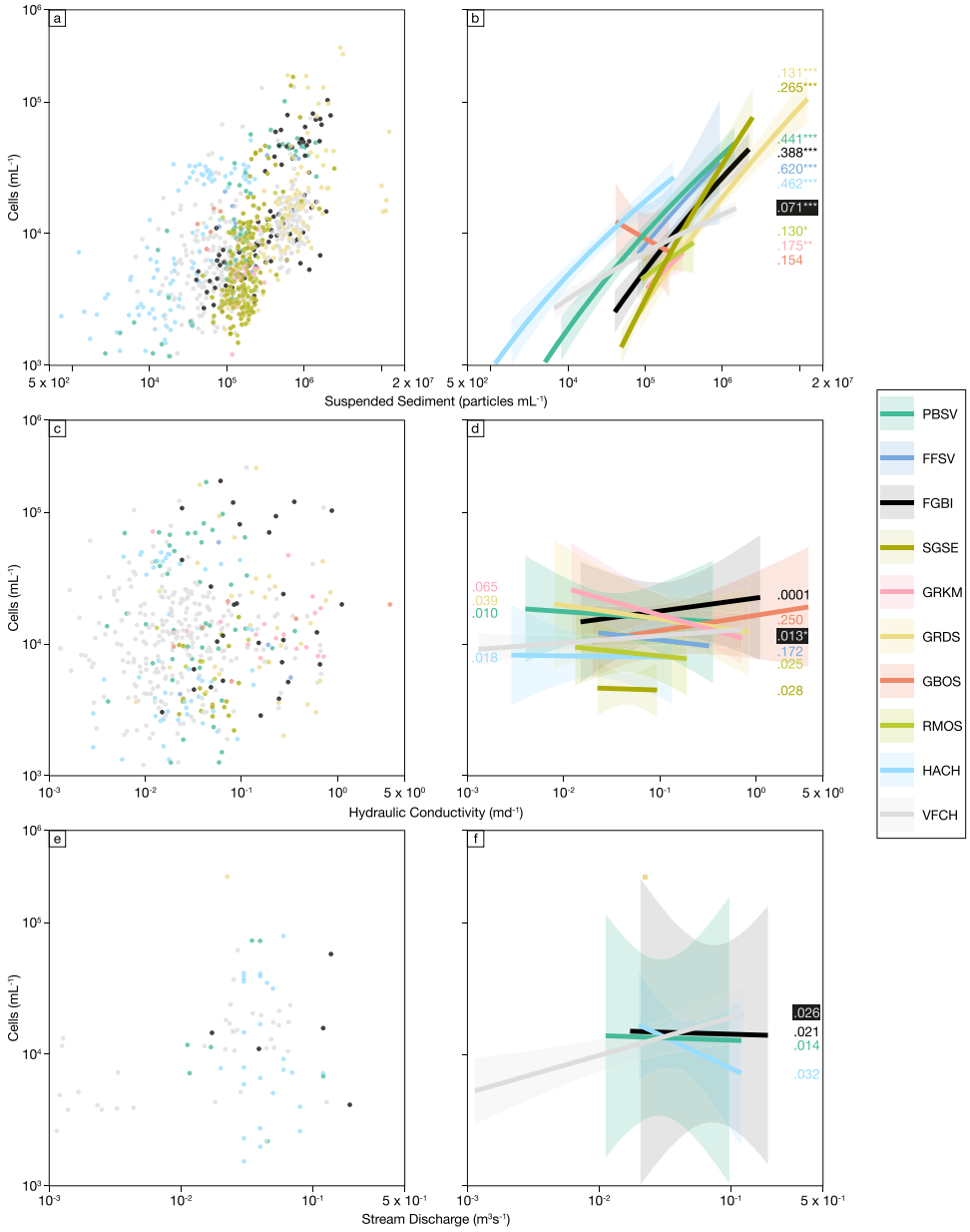

Fig. 4 Associations between cell concentration and related hydraulic variables. **a** Scatter plot of suspended sediment concentration (particles mL^{-1}) against cell concentration for all samples. **b** Linear regressions of suspended concentration against abundance for each glacier site. **c** Scatter plot of hydraulic conductivity (K) in m d^{-1} against cell concentration for all weathering crust samples. **d** Linear regressions for C. **e** Scatter plot of stream discharge (Q) in m^3 s^{-1} against cell concentration for four glacier settings where measurements $n > 5$. **f** Linear regressions for E. For all plots, each glacier's data are colour-coded; for plots **b**, **d**, and **f** the 95% confidence limits are shown, and adjusted r^2 values are given with significance indicated by * for $p < 0.1$, ** for $p < 0.05$, and *** for $p < 0.01$. Note that r^2 values for VFCH are presented with a black background for visual clarity.

absence of a more complete ecological understanding of the weathering crust, we assume that microbial community composition and abundance will not be modified over the next ~80 years. Moreover, it should be noted that these estimates represent a lower-end estimate of carbon export, due to the accuracy of the enumeration protocol (~84%; see Supplementary Information). We limit our upscaling to RGI regions 1–12, as this corresponds to regions which are either directly sampled in this study or are considered broadly glaciologically and/or climatically similar. Given the consistency in microbial abundance across the sampled glaciers, we consider the data collected in each region to provide suitable representation of the entire region, despite local differences in glacial settings and characteristics such as climate, slope, aspect, elevation, and mineralogy. Thus, there remains a paucity of data from glaciers in High Mountain Asia and the Southern Hemisphere, the study of which would further enhance our knowledge of supraglacial microbial fluxes. Consequently, the supraglacial carbon flux we present herein is not a global estimate, but the regions for which we project fluxes incorporate ~71% of the total projected RGI runoff.

Under a medium emission scenario (RCP 4.5), we forecast an annual average of 2.9×10^{22} cells yr^{-1}, equivalent to 0.65 Mt yr^{-1} of cellular carbon, will be exported from our study regions and the Greenland Ice Sheet (Fig. 5, Supplementary Table 6) during the 21st century. This is equivalent to between 10 and 15% of the POC flux from Arctic Rivers (5 ± 1 Mt C yr^{-1}; ref. [63]), and 0.4% of global biospheric river POC flux ($157 + 74/-50$ Mt C yr^{-1}; ref. [64]). Glaciers (c.f. the Greenland Ice Sheet) are the dominant

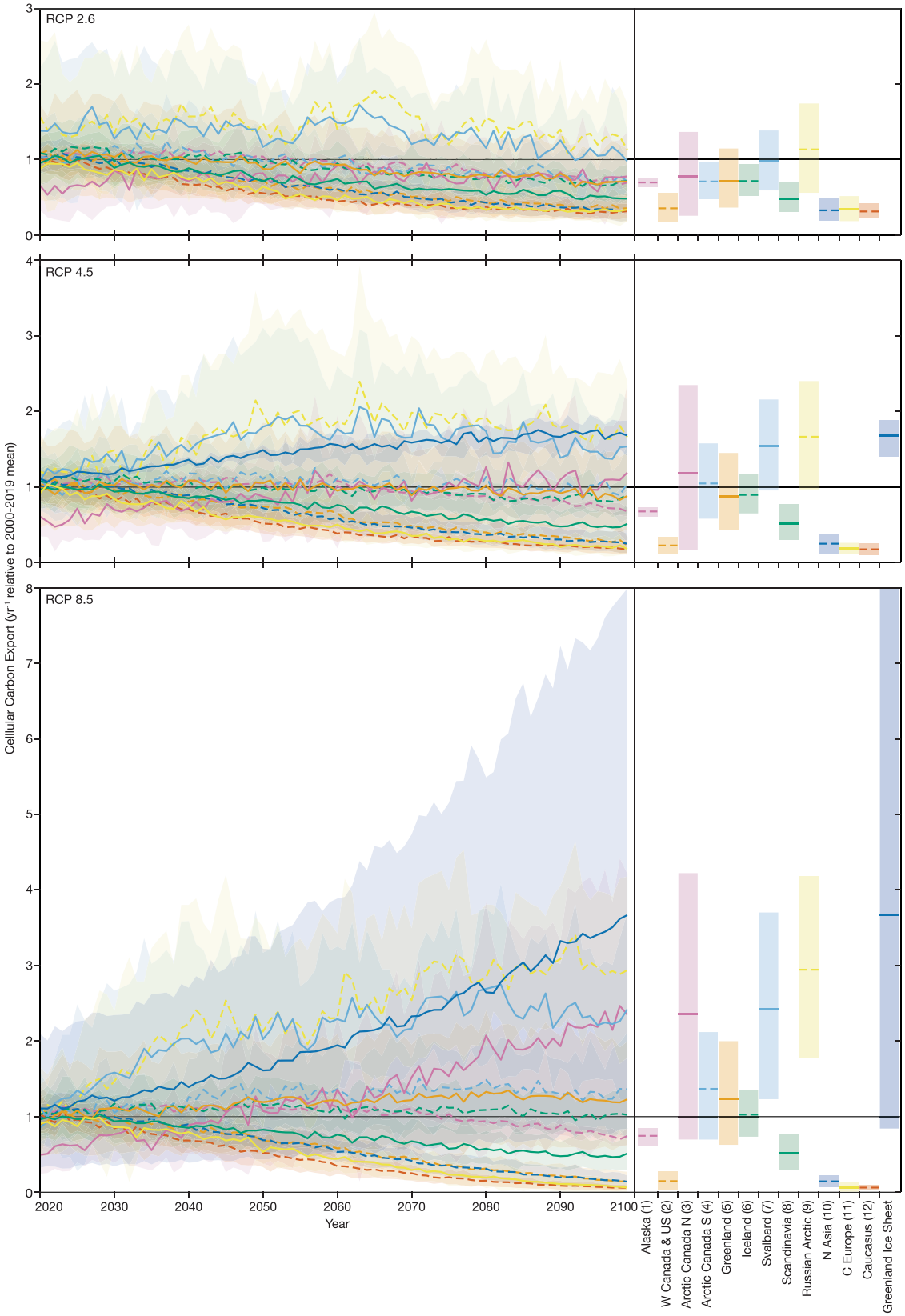

Fig. 5 Cellular carbon export trends under low, medium and high emissions scenarios (RCPs 2.6, 4.5 and 8.5) from 2020 to 2099, relative to the regional mean for 2000–2019. Note these trends also reflect relative changes in the absolute number of microbes exported. The right-hand panel depicts the mean and ± uncertainty in 2099 for the corresponding region. Note that there is no projection for the Greenland Ice Sheet under RCP 2.6. Solid lines indicate directly sampled regions, whilst dashed lines indicate extrapolated regions. Note that regions of equal colour are not connected in any fashion, the reuse of colour is a function of inherent colour palette limitations.

source of liberated cells and carbon (despite only representing a global sub-sample), delivering, on average, 1.8×10^{22} cells, or 0.40 Mt C yr^{-1}. Mirroring established discharge predictions[3], 'peak carbon' (i.e. maximal carbon export rate) from glaciers is reached between before 2040 under a low emissions scenario and between 2040 and 2059 under the medium emissions scenario. 'Peak carbon' will not be reached this century under a high emissions scenario, with end-of-century exports exceed 2000–2019 levels by 34% as glaciers continue to recede[65]. Within this first-order approximation, there are extreme regional differences (Fig. 5, Supplementary Table 6), most notably as glaciers in the mid-latitude/high altitude regions of Alaska, Western Canada/US, Scandinavia, North Asia, Central Europe and the Caucasus become diminished towards the end of the 21st century. Moreover, the Greenland Ice Sheet exhibits rising cellular carbon export under both medium and high emissions scenarios in our forecast, in contrast to glaciers under the medium emissions scenario, becoming an increasingly large contributor to total carbon export from glacierised catchments throughout the century.

The data herein do not allow a detailed prediction of the fate of this supraglacially derived carbon source. We assume, to facilitate discussion, that supraglacially derived cellular carbon is a) equivalent to total supraglacially derived POC and b) is efficiently advected from the supraglacial hydrological system to the en- and subglacial networks before delivery to downstream ecosystems and marine environments. Previous work suggests that POC delivered to downstream ecosystems from the Greenland Ice Sheet is derived primarily from rock and soil weathering in the subglacial system[66,67], with such material comprising 85 ± 5% of total proglacial POC[68] and the remainder (15 ± 5%) sourced directly from the ice surface. For the Greenland Ice Sheet, our observations broadly correspond with this assessment; surface cellular carbon export (0.18 Mt C yr^{-1}) is between 20 and 43% of the total forecast POC export for the ice sheet of 0.90 Mt C yr^{-1} (refs. [7,68] respectively). The implication of this numerical comparison is that there is little evidence for the processing or storage of supraglacial cellular carbon at the bed of the Greenland Ice Sheet during the ablation season, and this material is delivered efficiently downstream; however, this work only represents a first estimate of the liability of such POC and further work should look to directly pair surface and proglacial measurements.

In contrast we show that, for glaciers, supraglacial cellular carbon export represents ~56% of previous global glacier POC export[7] (0.39 of 0.70 Mt C yr^{-1}). Continuing the use of both assumptions used for the Greenland Ice Sheet, this proportional POC divide implies that cells from glacier surface are the primary source of glacially exported POC. We propose that surface-derived POC is a larger constituent of proglacially exported POC due to the relatively shorter subglacial drainage length at the glacial sites: we report a mean sample site-to-terminus distance of only 5 km (after refs. [69,70]) in contrast to flowpath lengths of 10–100 km long[71] for the Greenlandic sites which contribute to these data.

Consequently, our study emphasises the importance of the supraglacial environment as a source of OC released to downstream ecosystems[4,7,8,15] especially from glaciers, although this biomass may be augmented and modified during its transit through the subglacial system. Over the next ~80 years, our data highlights the strong potential for ecological change[4–6] in environments where glacial carbon export is predicted to increase (Arctic Canada, Greenland, Svalbard and the Russian Arctic), diminish (Western Canada and the US, Scandinavia and North Asia), or potentially disappear entirely (European Alps, Caucasus). Here we provide a critical baseline for the release of supraglacial cellular carbon and highlight the requirement for further exploration of the microbial ecology of supraglacial environments. Such understanding is essential to better understand the downstream biogeochemical implications of future glacial retreat under a changing climate.

Conclusions

Amidst the ongoing decline of mountain glaciers[2] and consequent modifications to meltwater runoff volume[3] and OC delivered to glacier-fed ecosystems[4,8], it is critical to advance the understanding glacier-derived carbon fluxes. Here, using samples form glacier and ice sheet surfaces around the Northern Hemisphere, we demonstrate the existence of an upper limit of microbial abundance in distributed and channelised glacial surface meltwaters of ~10^4 cells mL^{-1}. The controls upon microbial abundance and export remain unclear; with the interacting roles of nutrient availability, ecosystem interactions or other physical or glaciological controls providing avenues for further investigation. We forecast a mean annual export of 2.9×10^{22} cells yr^{-1}, equivalent to cellular carbon export of 0.65 Mt yr^{-1}, from glaciers (1.8×10^{22} cells or 0.40 Mt C yr^{-1}) in the Northern Hemisphere (except High Mountain Asia) and the Greenland Ice Sheet (1.1×10^{22} cells or 0.25 Mt C yr^{-1}) under a medium emission scenario, with marked declines in carbon export in mid-latitude montane glaciers over the next ~80 years. Moreover, we identify that supraglacial-derived cells comprise the majority of POC exported from glaciers outside the major ice sheets, and over 40% of POC exported from the Greenland Ice Sheet, highlighting the link between supraglacial microbial communities and downstream biogeochemical change under a warming climate. As such, it is essential to further understand the ecology of these microbial communities that live within and are exported from the supraglacial environment to fully comprehend the biogeochemical effects of climate change in soon-to-be deglacierised regions.

Materials and methods

Fieldwork was undertaken over a two-year period between July 2014 and July 2016. Ten sites across the northern hemisphere in contrasting latitudinal and climatological settings were sampled (Fig. 2; Supplementary Table 2). Field campaigns were conducted in the ablation area of each glacier/ice sheet location during the summer melt season, with sites selected to represent the wider glaciological landscape.

Enumeration of glacial microbes. Meltwater samples for microbial enumeration were collected from both weathering crust and stream environments. In the weathering crust, 15 mL of depth-integrated meltwater was extracted from auger holes following the collection of hydrological data, using a thrice pre-rinsed polyethylene syringe and 30 cm polypropylene tube. Of this, 10 mL was decanted into a 15 mL sterile screw-top centrifuge tube (Fischer Scientific; UK). Stream samples were collected directly in centrifuge tubes prior to stream discharge measurement. Both sample types were fixed using paraformaldehyde (samples collected at Vadrec del Forno, VFCH) or glutaraldehyde (both 2% w/v final concentration) and kept in the dark and cool (~ 4 °C) for up to 14 days before freezing for long term storage at −80 °C.

Samples were enumerated using an optimised flow cytometry (FCM) protocol as described in detail within the Supplementary information (Optimisation, evaluation and application of flow cytometry for microbial enumeration of glacial meltwater). Briefly, samples were thawed in the dark at ambient room temperature for ~16 h[35,72], vortexed for ≥30 s and divided into two 1 mL aliquots. One aliquot was stained with SYBR-Gold (Molecular Probes, UK) at a final concentration of 1×, whilst the other was left unstained. Aliquots were stored in the dark at 20 °C for a maximum of 240 min prior to enumeration. FCM analysis was undertaken using a Sony SH-800EC cell sorter (Sony Biotechnology, Japan) which was aligned and calibrate daily following the manufacturer's instructions. A minimum of 400 μL of each aliquot was analysed at a flow rate between 21 and 63 μL min^{-1}, depending on the event rate, itself proportional to the sediment and microbial concentration of each sample. Microbial counts were calculated by comparing the stained/unstained aliquot pairs using a multi-stage gating protocol: FSC-A/FSC-H was used to examine for aggregation, and FITC/BSC for identification of microbes. Cell sizes categories ranging from <1 to >15 μm were estimated using a non-fluorescent Flow Cytometry Size Calibration Kit (Molecular Probes, UK) following the manufacturer's instructions. Our size assessment was constrained by the instrumental 0.5 μm a detection limit. Due to the fixation of samples in the field

and use of the non-discriminatory stain SYBR Gold, we are unable to distinguish between viable and non-viable microbes using this protocol.

Weathering crust and stream hydrology. Weathering crust hydraulic conductivity was calculated using the bail-recharge method, employing 36 cm deep auger-holes of 5 cm diameter, drilled with a Kovacs ice auger (note that we refer to the ice auger, not a standard corer). Bespoke capacitance piezometers[23], yielding water level at 2 s intervals, were used to record auger-hole recharge. Piezometers were rinsed three times with supraglacial stream water prior to installation to minimise cross-contamination of the microbial samples. Hydraulic conductivity (K) was calculated from these recharge curves using standard groundwater techniques[73]. Auger-hole water temperature and EC were recorded using a combined Reed SD-4307 probe following microbial sample collection at HACH, PBSV and VFCH.

Supraglacial stream discharge was recorded at six sites (PBSV, FFSV, FGBI, SGSE, RMOS and HACH) using salt dilution gauging at a fixed location. At VFCH, a Druck pressure transducer was installed at a fixed in-stream location to measure stage at a one minute resolution, with data recorded using a Campbell CR1000. A stage-discharge relationship was established using spot discharge measurements using salt dilution gauging.

Cell and cellular carbon export from glacier surfaces. Cellular carbon export from all glacier surfaces and the Greenland Ice Sheet over the 21st century was estimated by upscaling averaged cellular carbon in supraglacial meltwaters at each glacier using modelled future glacial discharge under different Representative Concentration Pathways (RCPs). Cellular carbon content per unit meltwater volume was calculated using abundance-size derived cell biovolume and allometric conversion ratios[61,62], and this value (cellular carbon mL^{-1}) was upscaled to regional supraglacial carbon export by multiplication using the output of regional glacier melt models. A fully detailed method follows.

To calculate cellular carbon concentrations, single-cell carbon mass was first calculated for each cell size bin, using allometric biovolume-to-carbon conversion factors. It was assumed that FCM determined cell size was equal to cell length, and that every cell within a given size bin was of median length. For example, a cell in the 4–10 µm bin was assigned a length of 7 µm; 17.5 µm was defined as the median length for the open-ended upper bin. It was assumed that all cells <1 µm were spherical, that cells 1≤ and ≥10 µm were rod-shaped bacteria with length(L):width(W) ratios calculated per Eq. (1) (ref. [74]) and total biovolume (V) as per Eq. (2) (ref. [75]). Cells >10 µm were assumed to be rod-shaped algae with $L{:}W = 2.6$ (ref. [76]). Biovolume was converted to cellular carbon (M; femtograms, fg) using Eq.(3), where c and a are domain-dependant constants. For bacteria[77], $c = 162$ and $a = 0.91$, and for algae[62] $c = 109$ and $a = 0.991$.

$$W = 0.888L + 0.111 \quad (1)$$

$$V = \frac{\pi}{4} w^2 \left(L - \frac{w}{3}\right) \quad (2)$$

$$M = cV^a \quad (3)$$

Single cell carbon for each bin was expanded to a g L^{-1} estimate for each glacier by calculating mean and ±5% cell concentrations for each size bin and multiplying cell count by the cellular carbon of a single cell within the corresponding bin. Total cellular carbon within each size bin was then summed to provide a glacier-wide value of predicted cellular carbon per litre of surface meltwater. These were upscaled to predict annual supraglacial cellular carbon export by using glacier and ice sheet runoff projections. For all glaciers globally, annual water runoff at the temporally evolving glacier terminus was computed using the Global Glacier Evolution Model (GloGEM)[59] based on projections of 13 Global Circulation Models (GCMs) driven by RCP 2.6, 4.5, and 8.5 emissions scenarios. Results were aggregated to RGI regions and for the mean of the utilised GCMs. For the Greenland Ice Sheet, projections were obtained using the regional climate model MAR (Modèle Atmosphérique Régional), forced by output of three CIMP5 (Coupled Model Intercomparison Project Phase 5) GCMs driven by RCP 4.5 and 8.5[60].

Glaciers were linked with their corresponding regions, or extrapolations made to non-sampled regions based on climatological and glaciological setting. It was not deemed appropriate to extrapolate to RGI regions 13–19 (High Mountain Asia and the Southern Hemisphere), nor to consider the Antarctic Ice Sheet as no direct nor glaciological comparable observations of cellular concentrations are available in these regions. Within these regions, there are several factors which prevent justifiable extrapolation, which ultimately cause surface environments which differ significantly from the glaciers we surveyed directly. For example, glaciers in High Mountain Asia often have thick debris mantles in their ablation zones and as such have predominantly different surface processes from their clean ice counterparts[78]. Glaciers in the south-eastern Himalaya[79] and low-latitudes[80] are typically of the summer accumulation type, with large amounts of precipitation characterising the melt season.

It should be noted that it is assumed that all meltwater is produced on the surface, drains from the surface, and is efficiently advected to downstream environments; that 1 L of meltwater weighs 1 kg; and that the microbial concentration in glacial surface snow melt[81] is an equivalent order of magnitude to that in ice melt, and remains constant throughout the melt season. The latter assumption is based upon a paucity of season-long data, and greater understanding of seasonal variation in microbial concentration would enable refinement of the carbon export estimates presented herein.

Uncertainty ranges for microbial carbon exported are calculated using uncertainties of both variables (cell concentration and modelled discharge). For cell concentration, the mean value is supplemented with a lower and higher bound estimate of concentration, using the 16th and 84th percentiles (equivalent to 1 standard deviation in a normally distributed population). Using similar estimates of uncertainty from the runoff model outputs for each emissions scenario (see refs. [59,60]), low-low and high-high values of cellular carbon and meltwater production were combined to establish low and high estimates of cellular carbon export over the coming 80 years.

Reporting summary. Further information on research design is available in the Nature Portfolio Reporting Summary linked to this article.

Data availability

Data presented in this manuscript is available here: https://doi.org/10.5281/zenodo.7034224

Received: 15 May 2022; Accepted: 27 October 2022;
Published online: 10 November 2022

References

1. Slater, T. et al. Review article: Earth's ice imbalance. *Cryosphere* **15**, 233–246 (2021).
2. Hugonnet, R. et al. Accelerated global glacier mass loss in the early twenty-first century. *Nature* **592**, 726–731 (2021).
3. Huss, M. & Hock, R. Global-scale hydrological response to future glacier mass loss. *Nat. Clim. Change* **8**, 135–140 (2018).
4. Hotaling, S., Hood, E. & Hamilton, T. L. Microbial ecology of mountain glacier ecosystems: biodiversity, ecological connections, and implications of a warming climate. *Environ. Microbiol.* https://doi.org/10.1111/1462-2920.13766 (2017).
5. Milner, A. M. et al. Glacier shrinkage driving global changes in downstream systems. *Proc. Natl Acad. Sci.* **114**, 9770–9778 (2017).
6. Hopwood, M. J. et al. Review article: How does glacier discharge affect marine biogeochemistry and primary production in the Arctic? *Cryosphere* **14**, 1347–1383 (2020).
7. Hood, E., Battin, T. J., Fellman, J., O'Neel, S. & Spencer, R. G. M. Storage and release of organic carbon from glaciers and ice sheets. *Nat. Geosci.* **8**, 91–96 (2015).
8. Hood, E., Fellman, J. B. & Spencer, R. G. M. Glacier loss impacts riverine organic carbon transport to the ocean. *Geophys. Res. Lett.* **47**, e2020GL089804 (2020).
9. Singer, G. A. et al. Biogeochemically diverse organic matter in Alpine glaciers and its downstream fate. *Nat. Geosci.* **5**, 710–714 (2012).
10. Brighenti, S. et al. Ecosystem shifts in Alpine streams under glacier retreat and rock glacier thaw: a review. *Sci. Total Environ.* **675**, 542–559 (2019).
11. Stibal, M., Sabacka, M. & Zarsky, J. Biological processes on glacier and ice sheet surfaces. *Nat. Geosci.* **5**, 771–774 (2012).
12. Dancer, S. J., Shears, P. & Platt, D. J. Isolation and characterization of coliforms from glacial ice and water in Canada's High Arctic. *J. Appl. Microbiol.* **82**, 597–609 (1997).
13. Cameron, K. A., Müller, O., Stibal, M., Edwards, A. & Jacobsen, C. S. Glacial microbiota are hydrologically connected and temporally variable. *Environ. Microbiol.* **22**, 3172–3187 (2020).
14. Holland, A. T. et al. Dissolved organic nutrients dominate melting surface ice of the Dark Zone (Greenland Ice Sheet). *Biogeosciences* **16**, 3283–3296 (2019).
15. Irvine-Fynn, T. D. L. et al. Storage and export of microbial biomass across the western Greenland Ice Sheet. *Nat. Commun.* **12**, 3960 (2021).
16. Müller, F. & Keeler, C. M. Errors in short term ablation measurement on melting ice surfaces. *Anglais* **8**, 91–105 (1969).
17. Cook, J., Edwards, A., Takeuchi, N. & Irvine-Fynn, T. Cryoconite:The dark biological secret of the cryosphere. *Progr. Phys. Geogr.: Earth Environ.* **40**, 66–111 (2016).
18. Irvine-Fynn, T. D. L. & Edwards, A. A frozen asset: the potential of flow cytometry in constraining the glacial biome. *Cytometry A* **85**, 3–7 (2014).
19. Edwards, A. & Cameron, K. A. in *Psychrophiles: From Biodiversity to Biotechnology* (ed Rosa Margesin) 57–81 (Springer International Publishing, 2017).

20. Christner, B. C. et al. Microbial processes in the weathering crust aquifer of a temperate glacier. *Cryosphere* **12**, 3653–3669 (2018).
21. Koziol, K. A., Moggridge, H. L., Cook, J. M. & Hodson, A. J. Organic carbon fluxes of a glacier surface: a case study of Foxfonna, a small Arctic glacier. *Earth Surf. Process. Landforms* **44**, 405–416 (2019).
22. Barker, J. D., Sharp, M. J., Fitzsimons, S. J. & Turner, R. J. Abundance and dynamics of dissolved organic carbon in glacier systems. *Arctic, Antarct. Alpine Res.* **38**, 163–172 (2006).
23. Stevens, I. T. et al. Near-surface hydraulic conductivity of northern hemisphere glaciers. *Hydrol. Process.* **32**, 850–865 (2018).
24. Cook, J. M., Hodson, A. J. & Irvine-Fynn, T. D. L. Supraglacial weathering crust dynamics inferred from cryoconite hole hydrology. *Hydrol. Process.* https://doi.org/10.1002/hyp.10602. (2015).
25. Žebre, M. et al. 200 years of equilibrium-line altitude variability across the European Alps (1901−2100). *Clim. Dyn.* **56**, 1183–1201 (2021).
26. Noël, B. et al. Low elevation of Svalbard glaciers drives high mass loss variability. *Nat. Commun.* **11**, 4597 (2020).
27. Noël, B. et al. Six decades of glacial mass loss in the Canadian Arctic Archipelago. *J. Geophys. Res.-Earth* **123**, 1430–1449 (2018).
28. Whitman, W. B., Coleman, D. C. & Wiebe, W. J. Prokaryotes: the unseen majority. *Proc. Natl Acad. Sci.* **95**, 6578–6583 (1998).
29. Amato, P. et al. Bacterial characterization of the snow cover at Spitzberg, Svalbard. *FEMS Microbiol. Ecol.* **59**, 255–264 (2007).
30. Laurion, I., Demers, S. & Vezina, A. F. The microbial food web associated with the ice algal assemblage: biomass and bacterivory of nanoflagellate protozoans in Resolute Passage (High Canadian Arctic). *Mar. Ecol. Prog. Ser. Oldendorf* **120**, 77–87 (1995).
31. Felip, M., Sattler, B., Psenner, R. & Catalan, J. Highly active microbial communities in the ice and snow cover of high mountain lakes. *Appl. Environ. Microb.* **61**, 2394–2401 (1995).
32. Skidmore, M., Anderson, S. P., Sharp, M., Foght, J. & Lanoil, B. D. Comparison of microbial community compositions of two subglacial environments reveals a possible role for microbes in chemical weathering processes. *Appl. Environ. Microb.* **71**, 6986–6997 (2005).
33. Mindl, B. et al. Factors influencing bacterial dynamics along a transect from supraglacial runoff to proglacial lakes of a high Arctic glacier. *FEMS Microbiol. Ecol.* **59**, 307–317 (2007).
34. Irvine-Fynn, T. D. L. et al. Microbial cell budgets of an Arctic glacier surface quantified using flow cytometry. *Environ. Microbiol.* **14**, 2998–3012 (2012).
35. Stibal, M. et al. Microbial abundance in surface ice on the Greenland Ice Sheet. *Front. Microbiol.* **6** https://doi.org/10.3389/fmicb.2015.00225 (2015).
36. Williamson, C. J. et al. Ice algal bloom development on the surface of the Greenland Ice Sheet. *FEMS Microbiol. Ecol.* **94** https://doi.org/10.1093/femsec/fiy025 (2018).
37. Williamson, C. J. et al. Algal photophysiology drives darkening and melt of the Greenland Ice Sheet. *Proc. Natl Acad. Sci.* **117**, 5694–5705 (2020).
38. Säwström, C., Mumford, P., Marshall, W., Hodson, A. & Laybourn-Parry, J. The microbial communities and primary productivity of cryoconite holes in an Arctic glacier (Svalbard 79°N). *Polar Biol.* **25**, 591–596 (2002).
39. Anesio, A. M. et al. Carbon fluxes through bacterial communities on glacier surfaces. *Ann. Glaciol.* **51**, 32–40 (2010).
40. Hodson, A. J. et al. Glacial Ecosystems. *Ecol. Monogr.* **78**, 41–67 (2008).
41. Foreman, C. M., Sattler, B., Mikucki, J. A., Porazinska, D. L. & Priscu, J. C. Metabolic activity and diversity of cryoconites in the Taylor Valley, Antarctica. *J. Geophys. Res. Biogeosci.* **112**, G04S32 (2007).
42. Wientjes, I. G. M. et al. Carbonaceous particles reveal that Late Holocene dust causes the dark region in the western ablation zone of the Greenland ice sheet. *Anglais* **58**, 787–794 (2012).
43. Stibal, M. et al. Organic matter content and quality in supraglacial debris across the ablation zone of the Greenland ice sheet. *Ann. Glaciol.* **51**, 1–8 (2010).
44. McCutcheon, J. et al. Mineral phosphorus drives glacier algal blooms on the Greenland Ice Sheet. *Nat. Commun.* **12**, 570 (2021).
45. Telling, J. et al. Microbial nitrogen cycling on the Greenland Ice Sheet. *Biogeosciences* **9**, 2431–2442 (2012).
46. Rassner, S. M. E. et al. Can the bacterial community of a high arctic glacier surface escape viral control? *Front. Microbiol.* **7** https://doi.org/10.3389/fmicb.2016.00956 (2016).
47. Nicholes, M. J. et al. Bacterial dynamics in supraglacial habitats of the Greenland Ice Sheet. *Front. Microbiol.* **10** https://doi.org/10.3389/fmicb.2019.01366 (2019).
48. Karlstrom, L., Zok, A. & Manga, M. Near-surface permeability in a supraglacial drainage basin on the Llewellyn Glacier, Juneau Icefield, British Columbia. *Cryosphere* **8**, 537–546 (2014).
49. Mantelli, E., Camporeale, C. & Ridolfi, L. Supraglacial channel inception: modeling and processes. *Water Resour. Res.* **51**, 7044–7063 (2015).
50. Gokul, J. K. et al. Illuminating the dynamic rare biosphere of the Greenland Ice Sheet's Dark Zone. *FEMS Microbiol. Ecol.* **95** https://doi.org/10.1093/femsec/fiz177 (2019).
51. Hudleston, P. J. Structures and fabrics in glacial ice: a review. *J. Struct. Geol.* **81**, 1–27 (2015).
52. Mader, H. M., Pettitt, M. E., Wadham, J. L., Wolff, E. W. & Parkes, R. J. Subsurface ice as a microbial habitat. *Geology* **34**, 169–172 (2006).
53. Tedstone, A. J. et al. Algal growth and weathering crust state drive variability in western Greenland Ice Sheet ice albedo. *Cryosphere* **14**, 521–538 (2020).
54. Ali, P. et al. A Glacier bacterium produces high yield of cryoprotective exopolysaccharide. *Front. Microbiol.* **10** https://doi.org/10.3389/fmicb.2019.03096 (2020).
55. Dolev, M. B., Bernheim, R., Guo, S., Davies, P. L. & Braslavsky, I. Putting life on ice: bacteria that bind to frozen water. *J. R. Soc. Interface* **13**, 20160210 (2016).
56. Smith, H. J. et al. Biofilms on glacial surfaces: hotspots for biological activity. *npj Biofilms Microbiomes* **2**, 16008 (2016).
57. Cook, J. M. et al. Quantifying bioalbedo: a new physically based model and discussion of empirical methods for characterising biological influence on ice and snow albedo. *Cryosphere* **11**, 2611–2632 (2017).
58. Consortium, R. Randolph Glacier Inventory—A Dataset of Global Glacier Outlines: Version 6.0: Technical Report. (Global Land Ice Measurements from Space, Colorado, USA, 2017).
59. Huss, M. & Hock, R. A new model for global glacier change and sea-level rise. *Front. Earth Sci.* **3** https://doi.org/10.3389/feart.2015.00054 (2015).
60. Fettweis, X. et al. Estimating the Greenland ice sheet surface mass balance contribution to future sea level rise using the regional atmospheric climate model MAR. *Cryosphere* **7**, 469–489 (2013).
61. Bratbak, G. Bacterial biovolume and biomass estimations. *Appl. Environ. Microb.* **49**, 1488–1493 (1985).
62. Montagnes, D. J. S., Berges, J. A., Harrison, P. J. & Taylor, F. J. R. Estimating carbon, nitrogen, protein, and chlorophyll a from volume in marine phytoplankton. *Limnol. Oceanogr.* **39**, 1044–1060 (1994).
63. Dittmar, T. & Kattner, G. The biogeochemistry of the river and shelf ecosystem of the Arctic Ocean: a review. *Mar. Chem.* **83**, 103–120 (2003).
64. Galy, V., Peucker-Ehrenbrink, B. & Eglinton, T. Global carbon export from the terrestrial biosphere controlled by erosion. *Nature* **521**, 204–207 (2015).
65. Hock, R. et al. GlacierMIP—a model intercomparison of global-scale glacier mass-balance models and projections. *Anglais* **65**, 453–467 (2019).
66. Wadham, J. L. et al. Ice sheets matter for the global carbon cycle. *Nat. Commun.* **10**, 3567 (2019).
67. Cameron, K. A. et al. Meltwater export of prokaryotic cells from the Greenland ice sheet. *Environ. Microbiol.* https://doi.org/10.1111/1462-2920.13483 (2016).
68. Bhatia, M. P. et al. Organic carbon export from the Greenland ice sheet. *Geochim. Cosmochim. Acta* **109**, 329–344 (2013).
69. Maussion, F. et al. The Open Global Glacier Model (OGGM) v1.1. *Geosci. Model Dev.* **12**, 909–931 (2019).
70. WGMS. *Fluctuations of Glaciers Database*. (World Glacier Monitoring Service, 2021).
71. Chandler, D. M. et al. Rapid development and persistence of efficient subglacial drainage under 900 m-thick ice in Greenland. *Earth Planet. Sci. Lett.* **566**, 116982 (2021).
72. Santibanez, P. A., McConnell, J. R. & Priscu, J. C. A flow cytometric method to measure prokaryotic records in ice cores: an example from the West Antarctic Ice Sheet Divide drilling site. *Anglais* **62**, 655–673 (2016).
73. Stevens, I. T. et al. Near-surface hydraulic conductivity of northern hemisphere glaciers. *Hydrol. Process.* **32**, 850–865 (2018).
74. WQA. *Common Contaminants: Bacteria and Virus Issues*, <https://www.wqa.org/learn-about-water/common-contaminants/bacteria-viruses> (2018).
75. Saccà, A. Methods for the estimation of the biovolume of microorganisms: a critical review. *Limnol. Oceanogr. Methods* **15**, 337–348 (2017).
76. Di Mauro, B. et al. Glacier algae foster ice-albedo feedback in the European Alps. *Sci. Rep.* **10**, 4739 (2020).
77. Norland, S. in Handbook of Methods in Aquatic Microbial Ecology (eds Paul F. Kemp, Barry F. Shedd, Evelyn B. Sherr, & Jonathan J. Cole) (Lawrence Erlbaum, 1993).
78. Miles, K. E. et al. Hydrology of debris-covered glaciers in High Mountain Asia. *Earth-Sci. Rev.* **207**, 103212 (2020).
79. Bolch, T. et al. The state and fate of Himalayan glaciers. *Science* **336**, 310–314 (2012).
80. Ribstein, P., Tiriau, E., Francou, B. & Saravia, R. Tropical climate and glacier hydrology: a case study in Bolivia. *J. Hydrol.* **165**, 221–234 (1995).
81. Liu, Y. et al. Microbial diversity in the snow, a moraine lake and a stream in Himalayan glacier. *Extremophiles* **15**, 411 (2011).

Acknowledgements

The authors would like to acknowledge the following funding bodies for financial support enabling both field campaigns and laboratory analysis: Aberystwyth University (Department of Geography and Earth Sciences): URF ASPECT-12104 to TI-F and URF-12465-01 to T.O.H.; Climate Change Consortium for Wales: C3W Proof of Concept to T.I.-F.; Gilchrist Educational Trust: ASPECT Expedition to I.T.S.; EU F7 INTERACT: SCARFACE to T.I.-F. and A.E.; Higher Education Funding Council for Wales (HEFCW): Extreme Experiments Laboratory (Ex2EL) and Geo-Carb-Cymru to A.C.M. and A.E.; Natural Environment Research Council (NERC): NE/M021025/1 to T.I.-F. and NE/S001034/1 to A.E., A.C.M. and T.I.-F.; Natural Sciences and Engineering Research Council of Canada (NSERC) and Polar Continental Shelf Project (PCSP) to B.J.M.; Rolex Awards for Enterprise to J.M.C.; Royal Geographical Society: Postgraduate Research Grant to I.T.S. and Small Research Grant SRG8/16 to T.O.H.; Royal Society: RG130314 to A.E. and T.I.-F.; Scottish Arctic Club: ASPECT Expedition to I.T.S.; and Welsh Government and HEFCW: Sêr Cymru National Research Network (NRN) - Low Carbon, Energy and the Environment to A.C.M. and A.E. We are grateful to the many individuals who assisted us in the field and laboratory. Parks Canada and the Northern Scientific Training Program (NSTP) are thanked for supporting fieldwork on Bylot Island in 2014, and the Dark Snow Project for supporting work on the Greenland Ice Sheet in the same year. Support enabling the final production of this manuscript was provided by Newcastle University (I.T.S.) and the European Research Council Synergy Grant: DEEP PURPLE (856416) (I.T.S. and J.M.C.).

Author contributions

I.T.S. developed the study, collected field data, carried out laboratory and numerical analysis and wrote the manuscript. T.I.F. conceived the study, collected field data, secured funding and discussed results and manuscript content. A.E. conceived the study, collected field data, secured funding and discussed results and manuscript content. P.R.P. collected field data and supplied essential instrumentation. J.M.C. collected field data. T.O.H., B.J.M., and B.S. collected field data and secured funding. A.J.H. contributed to the early conceptualisation of the study and collected field data. A.M. secured funding and contributed to discussion of the results and final manuscript content. X.F. and M.H. provided hydrological modelling data for carbon export upscaling. All authors contributed to final manuscript development.

Competing interests

The authors declare no competing interests.

Additional information

Supplementary information The online version contains supplementary material available at https://doi.org/10.1038/s43247-022-00609-0.

Correspondence and requests for materials should be addressed to Ian T. Stevens.

Peer review information *Communications Earth & Environment* thanks A. Ramanathan and the other, anonymous, reviewer(s) for their contribution to the peer review of this work. Primary Handling Editors: Ilka Peeken and Clare Davis. Peer reviewer reports are available.

Reprints and permission information is available at http://www.nature.com/reprints

Publisher's note Springer Nature remains neutral with regard to jurisdictional claims in published maps and institutional affiliations.

Open Access This article is licensed under a Creative Commons Attribution 4.0 International License, which permits use, sharing, adaptation, distribution and reproduction in any medium or format, as long as you give appropriate credit to the original author(s) and the source, provide a link to the Creative Commons license, and indicate if changes were made. The images or other third party material in this article are included in the article's Creative Commons license, unless indicated otherwise in a credit line to the material. If material is not included in the article's Creative Commons license and your intended use is not permitted by statutory regulation or exceeds the permitted use, you will need to obtain permission directly from the copyright holder. To view a copy of this license, visit http://creativecommons.org/licenses/by/4.0/.

© The Author(s) 2022